HIGH-EFFICIENCY CHROME TANNING USING PRE-TREATMENTS: SYNCHROTRON SAXS AND DSC STUDY

Yi Zhang, Jenna K. Buchanan, Geoff Holmes and Sujay Prabakar[a]

Leather and Shoe Research Association of New Zealand, P.O. Box 8094, Palmerston North, 4472, New Zealand

a) Corresponding author: sujay.prabakar@lasra.co.nz

Abstract. Pre-treatments are widely used during tanning processes to improve the performance of the main tannage. To study the effect of each type of pre-treatment on chromium-collagen cross-linking reaction during tanning, synchrotron small-angle X-ray scattering (SAXS) and differential scanning calorimetry (DSC) were used to provide fundamental understanding of the overall performance of each process. Four common types of pre-treatment were investigated in this study: monodentate complexing agent (sodium formate, SF), chelating agent (disodium phthalate, DSP), covalent cross-linker (glutaraldehyde, GA) and nanoclay (sodium montmorillonite, MMT). Based on the structural and thermal analyses, the performance of chrome tanning with pre-treatments was presented considering five aspects: cross-linking, the level of hydration, hydrothermal stability, uniformity through leather cross-section and the uptake of chrome. At the same chrome offers, leather pre-treated using SF, DSP and MMT showed improved hydrothermal stability, uniformity and level of hydration, while GA showed decreased hydration. All of the pre-treatments reduce surface fixation by decreasing the reactivity of chromium with collagen. Insights into the structural changes of collagen during tanning with varied reaction conditions can guide the design of novel, benign tanning processes to reduce environmental impact.

1 Introduction

Pre-treatments such as masking or pre-tanning modify the collagen structure in skins and hides to improve the efficiency of the main tannage.[1] Chrome is one of the most common main tannages which is involved in around 90% of the world's leather production.[2-3] However, its usage during tanning is so far inefficient, considering its excess usage to meet with the demanded production rate, leading to poorer uptake with the remainder discharged to the effluent.[2, 4] Many types of pre-treatments have been applied in chrome tanning to compensate for its weaknesses in efficiency via different mechanisms including complexing (masking), covalent cross-linking (pre-tanning) and electrostatic binding (filling or coating).[1] However, the molecular-level structure of collagen affected during the pre-treatments and chrome tanning are yet to be clarified.

Small-angle X-ray scattering (SAXS) has been applied to study the long-range ordered collagen structure in untanned skins and hides as well as leathers.[5-9] During leather processing, the collagen fibrils in skins and hides showed significant changes that can be monitored using synchrotron-based SAXS. Differential scanning calorimetry (DSC) is used in combination with SAXS to study the hydrothermal stability of collagen in leather to provide an all-round image of the characteristic performance of each pre-treatment method. In this study, four mainstream pre-treatments were selected to represent different mechanisms including sodium formate (SF) as a monodentate complexing agent, disodium phthalate (DSP) as a chelating agent, glutaraldehyde (GA) as a covalent cross-linker, and sodium montmorillonite (MMT) as a nanofiller. A high-exhaustion chrome tanning process, "ThruBlu", was chosen as a model to highlight differences across the pre-treatments. The aim of this study is to establish an overall understanding of pre-treatments about their interactions with collagen and/or chromium, as well as the resulting properties of the leather products.

2 Materials and Methods

2.1 Leather processing

Pickled grain splits of cattle hide were processed using modified ThruBlu chrome tanning.[7] Sodium bicarbonate was added to raise the pH to 7.5-8.0 before tanning. The pH is brought down to 4.0 by the acidity of chrome at the end of overnight processing.

For GA sample: pickled hides (uncross-linked hide, Col) were treated with 2.0% offer of 50% glutaraldehyde aqueous solution followed by neutralisation (Col-GA).

For other samples: pickled hides were neutralised (Col-STD), and then treated by different pre-treatments: 2.5% of Feliderm® DP solution (Col-DSP), 0.5% sodium formate (Col-SF) or 2.0% Cloisite® Na+ Nanoclay (Col-MMT).

Pre-treated samples were then tanned with Chromosal® B (basic chromium sulphate) at 3.0%, 4.5%, 6.0% offers overnight (named as Cr-1, Cr-2 and Cr-3, respectively). The wet blue leathers were then stored in a fridge (4°C) ready for further analyses.

2.2 Structural analysis using SAXS

Thin slices of hide samples were prepared using a microtome (Leica CM1850 UV, Leica Biosystems) to the same section size of 0.3 cm × 0.3 cm × 200 µm (L × W × H). Such slices were collected across grain, centre and corium layers of the leather cross-section and then air-dried at room temperature prior to SAXS measurement. SAXS measurements were carried out at beamline I22 at the Diamond Light Source. Dry leather slices were held between Kapton® tape to keep the moisture levels constant. The measurements were taken using 12.4 keV X-rays with a 9.7m sample-to-detector distance. The images were processed to q-plot ($q = 0.021 - 1.7 nm^{-1}$) using Data Analysis WorkbeNch (DAWN).[10] SAXS data were then fitted to a combined population and fibre d-spacing model implemented using SAXSFit.[11] Relative peak intensity is calculated as $R_{i/j}=A_i/A_j$, where A_i stands for the area of peak order i.

2.3 Hydrothermal analysis using DSC

Samples were microtomed and rehydrated with DI water in sealed Tzero aluminium pans overnight, followed by ramping at 5°C/min from 30°C to 120°C under N_2 purge (DSC Q2000, TA Instruments). The temperature of the onset of the peaks on DSC curves were calculated as the denaturation temperature (T_d) of the hide sample. By carrying out measurements throughout the cross-section of leather, the lowest and highest T_d (i.e., T_{min} and T_{max}) were determined ($T_d = T_{min}$). The range of T_d across the cross-section of each hide was calculated as: $R_T = T_{max} - T_{min}$.

2.4 Chrome uptake analysis using AAS

The percentage uptake of chrome (Up%) in leather samples as measured by Atomic absorption spectrophotometer (AAS) (SpectrAA 220FS, Varian). First, leather samples were hydrolysed using an excess amount of concentrated nitric acid and a mixture of perchloric acid and sulphuric acid to solubilise chromium species. Then, the mixtures were diluted with water followed by boiling for at least 10 min to eliminate the unreacted oxidising acids. The solutions were filtered and further diluted to an optimal concentration for AAS measurements (air/acetylene flame, wavelength = 357.9 nm, spectral bandwidth = 0.2 nm). Percentage uptake was then calculated as: Up% = 100% * (the amount of chromium in the leather after processing) / (the amount of chromium added during processing).

2.5 Overall performance

Overall performance of each pre-treatment method was compared according to the average ranking of (1) $R_{3/2}$; (2) T_d and (3) Up% by descending order, and (4) $R_{6/8}$ and (5) R_T by ascending order, of samples tanned with all three chrome offers.

3 Results and Discussions

3.1 SAXS: Structural analysis

Small-angle X-ray scattering of the standard chrome tanned hide sample showed a characteristic scattering pattern of fibrillar collagen (Fig. 1a), which originates from the long-range ordered packing of collagen molecules. The packing of collagen in hides follows a quarter-staggered arrangement with axial gap/overlap regions in a characteristic axial periodicity (D-period).[12] Due to the variation of electron density across the hide collagen matrix, the intensity of diffraction rings in the SAXS image changes amongst different orders.[13] Therefore, SAXS allows us to study collagen structural changes during chemical cross-linking that disrupts the electron density distributions in the matrix. Tanning with 3.0%, 4.5% and 6.0% chrome offers (named as Cr-1, Cr-2 and Cr-3) changes the intensity of the diffraction peaks significantly (Fig. 1b).

To highlight the changes of each order peaks, the normalised intensity of all peaks was plotted across different processing stages (Fig. 2). While the 1st and 2nd order peaks showed a drastic decrease in intensity, the other peaks (3rd to 9th) increased to different extents. The overall peak intensity changes could be attributed to: (i) the enhanced electron density contrast due to the introduced chromium species to the matrix; (ii) the structural changes triggered by chromium-collagen covalent and non-covalent interactions.

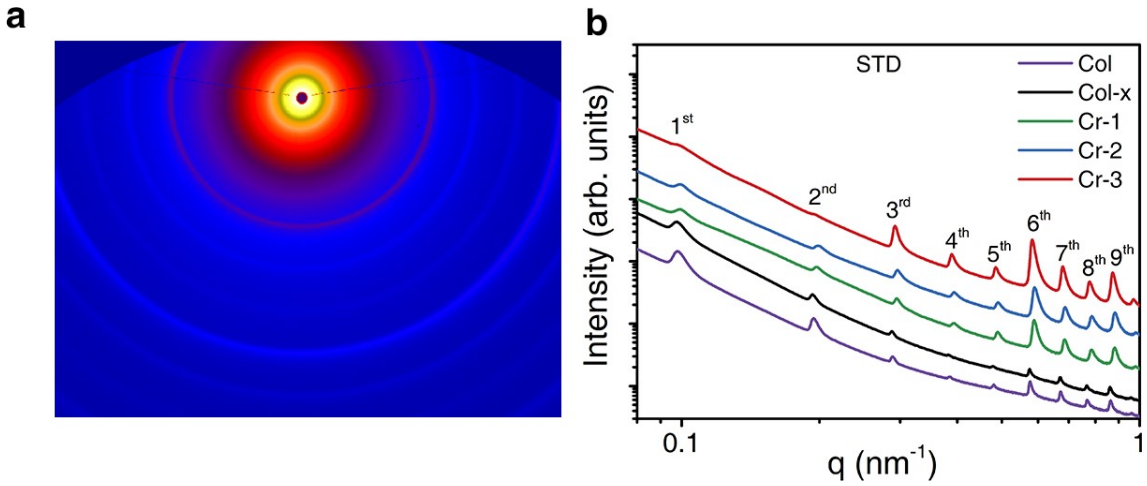

Fig. 1. (a) 2D SAXS image of chrome tanned leather. (b) Integrated 1D SAXS plots of untanned hide (Col), pre-treated hide through standard method (Col-x, where x = STD) and the subsequent chrome tanned leather (Cr-1, Cr-2 and Cr-3). Diffraction peaks are labelled according to q = 2πn/D where n is the peak order and D is the D-period. © Int. J. Biol. Macromol. DOI: 10.1016/j.ijbiomac.2018.12.187.

Similar observations on the changes in peak intensity before and after tanning has been reported on both skins and hides from the 4th to 9th order peaks.[6-7, 14] However, the 3rd order peak has shown a decrease in wet leather after chrome tanning,[7] unlike what we have found in this study using dry leather. Previous reports showed that during drying, the intermolecular structure of collagen contracts and caused a decrease in the 3rd order peak,[15] while cross-linking can provide resistance

to contraction, resulting in a stronger 3rd order peak in a dry state. Instead, the uncross-linked collagen can contract without the introduced restrictions to give a weaker 3rd order peak. On the other hand, a larger increase in the 6th order peak along with the increase in chrome offer was also observed over the other order peaks (Fig. 2). Stronger 6th order peak compared to the 3rd, 5th, 7th or 8th as previously found to relate to the drying of collagen.[14-16] In this study, all samples have been dried equally in air at room temperature, so that the intensity changes of 6th over the other peaks showed insightful evidence into the binding environment of water with collagen, which varies amongst the different pre-treatments.

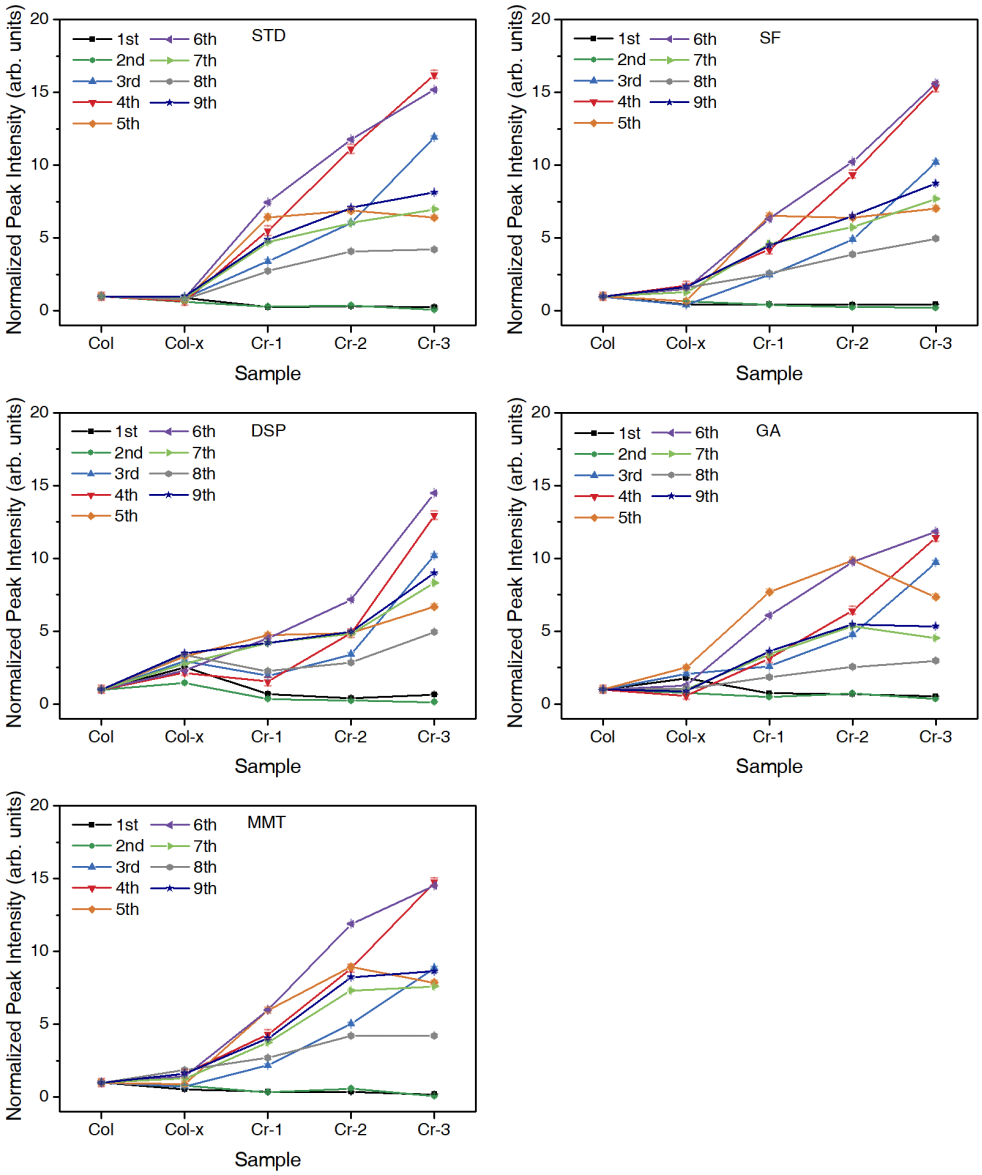

Fig. 2. Normalized 1st to 9th order peak intensity of each sample at different processing stages: untanned hide (Col), pre-treated hide (Col-x, x = STD, SF, DSP, GA and MMT) and the subsequent chrome tanned leather (Cr-1, Cr-2 and Cr-3). © Int. J. Biol. Macromol. DOI: 10.1016/j.ijbiomac.2018.12.187.

To study the effect of chromium cross-linking on collagen structure with various pre-treatments, the relative diffraction peak intensities of the 3rd to 2nd ($R_{3/2}$) and the 6th to 8th ($R_{6/8}$) order peaks (Fig. 3). $R_{3/2}$ indicates variations in the axial gap/overlap region of the collagen molecules, allowing investigation of the structural resistance to osmotic shrinkage.[17] On the other hand, $R_{6/8}$ indicates

the level of hydration of the collagen molecules, which can affect the organoleptic properties of the leather products.[17-18]

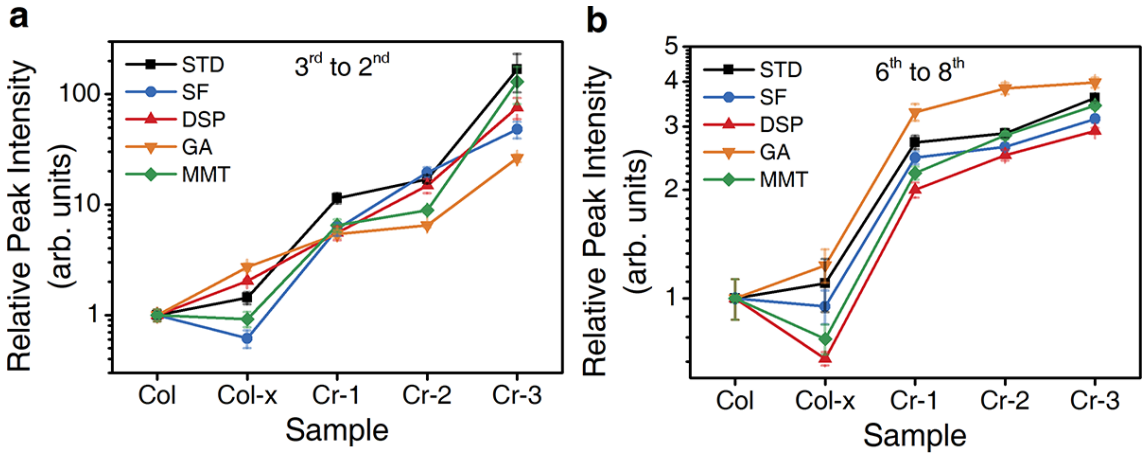

Fig. 3. Relative intensity ($R_{i/j}$, where i, j as peak orders) of (a) 3rd to 2nd and (b) 6th to 8th order peak of different samples: untanned hide (Col), pre-treated hide (Col-x, x = STD, SF, DSP, GA and MMT) and the subsequent chrome tanned leather (Cr-1, Cr-2 and Cr-3). © Int. J. Biol. Macromol. DOI: 10.1016/j.ijbiomac.2018.12.187.

3.1.1 Cross-linking performance

One of the most important indicators of a successful tanning process is the cross-linking performance, which is revealed using $R_{3/2}$. According to the results (Fig. 3a), the pre-treatment step caused significant changes in $R_{3/2}$. GA caused the biggest change and this can be explained by its covalent cross-linking mechanism.[1, 19] The other pre-treatments caused lesser changes in $R_{3/2}$ due to the non-covalent nature of their interactions with collagen.[1, 20-22] After chrome tanning, all samples saw a significant increase in $R_{3/2}$. The covalent cross-linking of chromium with collagen constrained its intermolecular structure, thereby causing less fibril contraction when unbound water was removed.[23] The lower $R_{3/2}$ of GA samples after chrome tanning implied a minimised cross-linking effect from chromium, due to the more confined collagen structure after first covalently cross-linking it with GA.[24] Although higher than the GA samples, the $R_{3/2}$ of SF, DSP and MMT samples were also lower compared to STD samples after chrome tanning. This is in good agreement with their mechanisms: SF and DSP complex with chromium to reduce its cross-linking effect, while MMT has negatively charged silanol ($Si\text{-}O^-$) and aluminol ($Al\text{-}O^-$) groups that can also mask chromium species by binding electrostatically.[1, 21-22]

3.1.2 Molecular hydration

Another performance indicator for the effect of chrome tanning, the molecular hydration of collagen, was demonstrated using $R_{6/8}$ (Fig. 3b). GA samples observed a higher $R_{6/8}$ over STD samples, confirming its covalent cross-linking mechanism that can lead to a decrease in hydrogen bonding sites in collagen and therefore, causes a less hydrated molecular structure.[25] Instead, SF, DSP and MMT brought carboxyl and hydroxyl groups into the collagen matrix and caused increased molecular hydration.[26-27] When tanned using a low chrome offer (Cr-1), $R_{6/8}$ increased significantly and then plateaued at high offers (Cr-2 and Cr-3), implying decreasing efficiency per unit of chromium on its covalent cross-linking with collagen due to the shortage of active sites at the high chrome offers.[7]

3.2 DSC: Hydrothermal stability

DSC analyses of pre-treated and chrome tanned hide samples also provided important performance indicators such as hydrothermal stability and uniformity (Fig. 4).

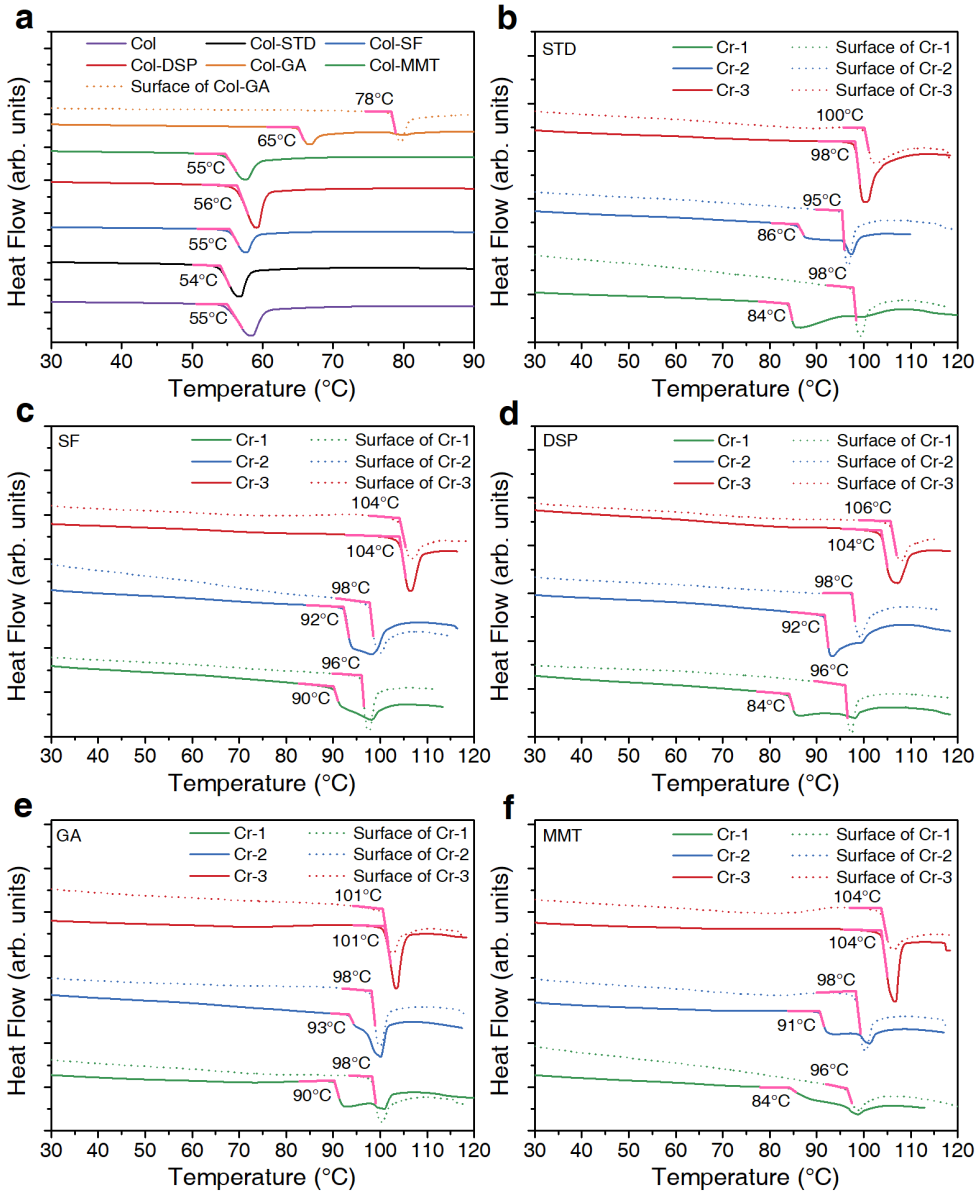

Fig. 4. DSC results of untanned hide (Col), pre-treated hide (Col-x, x = STD, SF, DSP, GA and MMT) and the subsequent chrome tanned leather (Cr-1, Cr-2 and Cr-3) throughout cross-sections (solid) or on the surfaces of the grain split hides (dotted). © Int. J. Biol. Macromol. DOI: 10.1016/j.ijbiomac.2018.12.187.

3.2.1 Hydrothermal stability

The most heat labile region of a tanned leather determines its overall denaturation temperature (T_d), which is also the minimum T_d throughout the cross-section of leather (T_{min}). Fig. 4a showed that there are only minor changes during pre-treatment using STD, SF, DSP and MMT, agreeing with their non-covalent interactions with collagen. On the other hand, covalent cross-linker, GA, caused an increment of T_d to 65°C. After chrome tanning (Fig. 4b-f), T_d increased significantly but the shapes

of endothermic peaks were different via each pre-treatment. Broad irregular shaped peaks were observed at low chrome offers (Cr-1 and Cr-2), while a high offer (Cr-3) produced sharper peaks. This highlighted the non-uniform penetration of chromium through the leather matrix.

Amongst all of the Cr-1 samples, a higher T_d at 90°C as observed in SF and GA samples, while MMT and DSP showed similar T_d at 84°C to the STD sample. Better penetration of chrome to the centre of the hide would provide a higher overall T_d of the collagen in leather. The masking effect of SF is again confirmed to assist the penetration of chrome. GA, on the other hand, limits the reaction of chromium with collagen on the surface via covalent cross-linking so as to improve the penetration. MMT and DSP samples showed no improvement in T_d in the centre, however, the shape of the endothermic peaks suggested a better distribution of chrome through the matrix. Stronger heat absorption at higher temperatures indicated a greater proportion of the collagen had improved hydrothermal stability. MMT can bind with chromium via electrostatic interactions to minimise the rapid cross-linking reaction to facilitate penetration. DSP contributed to penetration via bulk chelation with chromium to reduce its affinity to collagen.

Cr-2 samples showed higher T_d than Cr-1 samples with narrowed endothermic peaks. In addition, all of the pre-treated samples exhibited better hydrothermal stability than STD. Although the T_d were very similar among the different pre-treatments, the shape of the endothermic peaks varied. The GA sample displayed the largest proportion of higher T_d collagen, followed by MMT, SF and DSP, in descending order.

Similarly, in Cr-3 samples, the T_d of pre-treated leather is higher than the standard. However, GA produced the lowest T_d (101°C) amongst the four pre-treatments, which could be attributed to its nature of covalent cross-linking that hindered chromium from reacting with the collagen.

3.2.2 Uniformity through leather cross-section

Surfaces of leather were also measured for their T_d to identify the T_{max} throughout the leather cross-section, and their uniformity can be calculated based on the difference between T_{min} and T_{max} (R_T). A large R_T value (i.e., a wide range of T_d across the cross-section) indicates non-uniform penetration of chromium through the leather. Across the three chrome offers, the lowest overall R_T was observed in SF and GA treated samples. DSP and MMT also showed a slight improvement to R_T compared with STD. The overall results of R_T were generally consistent with improvements at low chrome offer.

3.3 AAS: percentage uptake of chrome

AAS analyses were conducted to quantify the uptake of chrome (Up%) for all pre-treatment methods (Table 1). In general, higher chrome offer was found to lead to a lower uptake, which agrees with previous observations. The percentage uptake of chromium was found to decrease with increasing chromium concentration, and is also in agreement with previous observations.[7]

Table 1. Percentage uptake of chrome during processing with different pre-treatments.

Chrome offer (%)	Chrome uptake (%)				
	STD	SF	DSP	GA	MMT
3.0 (Cr-1)	92 ± 2	84 ± 2	84 ± 1	99 ± 4	92 ± 2
4.5 (Cr-2)	82 ± 2	78 ± 2	76 ± 1	85 ± 1	81 ± 3
6.0 (Cr-3)	70 ± 2	61 ± 2	71 ± 2	67 ± 1	77 ± 2

GA provided an increased uptake compared to STD, whilst SF and DSP reduced uptake. GA improves chrome uptake at lower offers by facilitating more uniform penetration through the leather. However, its cross-linking also hinders the reaction of collagen with chromium at high offers therefore resulting in a lower uptake. SF and DSP complex with chromium to decrease its affinity

and ability to fix to the collagen molecules, hence providing reduced overall uptakes of chromium. MMT mitigates the reaction of chromium with collagen via its preferential adsorption of chromium species. Due to the affinity of chromium to collagen, it balances and prefers to fix to collagen at the end of the tanning process. In the presence of an excess of chrome, the active sites on collagen can be exhausted; with the rest of the chromium species therefore being adsorbed onto the MMT, resulting in a higher uptake in the highest chrome offer.

3.4 Overall performance of pre-treatments

The overall performance of four common pre-treatments was summarised according to their rankings across five key aspects. Cross-linking ($R_{3/2}$) and hydration ($R_{6/8}$) can greatly affect the organoleptic properties of leather. Hydrothermal stability (T_d) is also crucial, especially for the manufacturing of shoes. When it comes down to the practical manufacturing, the uptake of chrome (Up%) and its uniformity through the leather cross-section also needs to be considered to balance the cost and production efficiency. An evaluation is therefore demonstrated based on five aspects (Fig. 5). SF, DSP and MMT reduced chromium-collagen cross-linking and increased molecular hydration, hydrothermal stability and uniformity. GA introduced a decrease in both chromium-collagen cross-linking and hydration by covalently cross-linking with the collagen. The uptakes of chrome were improved by GA cross-linking and MMT adsorption. However, uptakes were reduced due to the complexing effect of either SF or DSP.

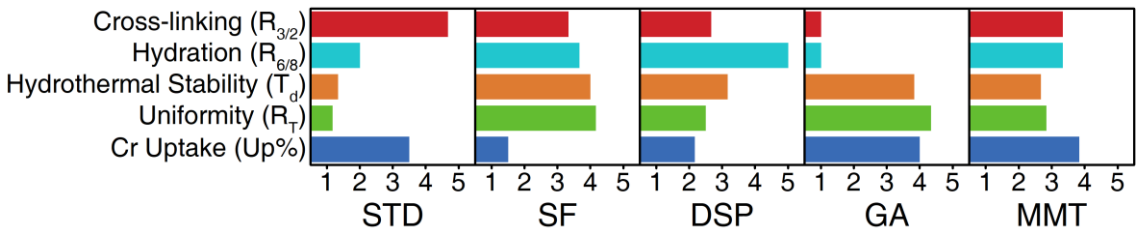

Fig. 5. Key aspects of the efficiency of chrome tanning through different pre-treatments. © Int. J. Biol. Macromol. DOI: 10.1016/j.ijbiomac.2018.12.187.

4 Conclusion

An efficient chrome tanning process can lead to a both economically and environmentally sustainable leather industry. Knowing the influence on performance of pre-treatments will allow us to improve the efficiency of chrome tanning, thereby improving collagen stability and the organoleptic properties of treated leather, alongside a reduction in chrome usage, mitigated environmental burden and diminished cost for the treatment of effluent. Our fundamental studies using SAXS and DSC provide a strategic guide to screen different combination tannages to design a more efficient chrome tanning processes. Such metrics can also be applied to the evaluation of cross-linkers for the biomedical industry to gauge their influence on collagen structure and hydrothermal stability.

5 Acknowledgements

S.P, Y.Z & G.H would like to thank the Ministry of Business, Innovation and Employment (MBIE) for providing funding through grant LSRX-1801. S.P & Y.Z would like to thank the Diamond Light Source, UK, for the granted access to SAXS beam time on the I22 beamline for this research.

References

1. *Covington, A. D.: Tanning chemistry: the science of leather, Royal Society of Chemistry: Cambridge, 2009.*
2. *Sreeram, K.; Ramasami, T.: 'Sustaining tanning process through conservation, recovery and better utilization of chromium', Resources, conservation and recycling, 38, 185-212, 2003.*
3. *UNIDO Future Trends in the World Leather and Leather Products Industry and Trade; UNIDO: Vienna, 2010; pp 1-120.*
4. *Sundar, V.; Rao, J. R.; Muralidharan, C.: 'Cleaner chrome tanning—emerging options', Journal of cleaner production, 10, 69-74, 2002.*
5. *Zhang, Y.; Ingham, B.; Leveneur, J.; Cheong, S.; Yao, Y.; Clarke, D. J.; Holmes, G.; Kennedy, J.; Prabakar, S.: 'Can sodium silicates affect collagen structure during tanning? Insights from small angle X-ray scattering (SAXS) studies', RSC Advances, 7, 11665-11671, 2017.*
6. *Zhang, Y.; Ingham, B.; Cheong, S.; Ariotti, N.; Tilley, R. D.; Naffa, R.; Holmes, G.; Clarke, D. J.; Prabakar, S.: 'Real-Time Synchrotron Small-Angle X-ray Scattering Studies of Collagen Structure during Leather Processing', Industrial & Engineering Chemistry Research, 57, 63-69, 2018.*
7. *Zhang, Y.; Mansel, B. W.; Naffa, R.; Cheong, S.; Yao, Y.; Holmes, G.; Chen, H.-L.; Prabakar, S.: 'Revealing Molecular Level Indicators of Collagen Stability: Minimizing Chrome Usage in Leather Processing', ACS Sustainable Chemistry & Engineering, 6, 7096-7104, 2018.*
8. *Naffa, R.; Maidment, C.; Ahn, M.; Ingham, B.; Hinkley, S.; Norris, G.: 'Molecular and structural insights into skin collagen reveals several factors that influence its architecture', International journal of biological macromolecules, 128, 509-520, 2019.*
9. *Zhang, Y.; Snow, T.; Smith, A. J.; Holmes, G.; Prabakar, S.: 'A guide to high-efficiency chromium (III)-collagen cross-linking: Synchrotron SAXS and DSC study', International journal of biological macromolecules, 126, 123-129, 2019.*
10. *Pauw, B. R.; Smith, A.; Snow, T.; Terrill, N.; Thünemann, A. F.: 'The modular small-angle X-ray scattering data correction sequence', Journal of applied crystallography, 50, 1800-1811, 2017.*
11. *Ingham, B.; Li, H.; Allen, E. L.; Toney, M. F.: 'SAXSFit: A program for fitting small-angle X-ray and neutron scattering data', arXiv:0901.4782, 1-5, 2009.*
12. *Petruska, J. A.; Hodge, A. J.: 'A subunit model for the tropocollagen macromolecule', Proceedings of the National Academy of Sciences, 51, 871-876, 1964.*
13. *Hulmes, D. J.; Miller, A.; White, S. W.; Doyle, B. B.: 'Interpretation of the meridional X-ray diffraction pattern from collagen fibres in terms of the known amino acid sequence', Journal of molecular biology, 110, 643-666, 1977.*
14. *Maxwell, C. A.; Smiechowski, K.; Zarlok, J.; Sionkowska, A.; Wess, T. J.: 'X-ray studies of a collagen material for leather production treated with chromium salt', Journal of the American Leather Chemists Association, 101, 9-17, 2006.*
15. *Fratzl, P.; Daxer, A.: 'Structural transformation of collagen fibrils in corneal stroma during drying. An x-ray scattering study', Biophysical Journal, 64, 1210-1214, 1993.*
16. *Tomlin, S.; Worthington, C. In Low-angle X-ray diffraction patterns of collagen, Proceedings of the Royal Society of London A: Mathematical, Physical and Engineering Sciences, The Royal Society: 1956; pp 189-201.*
17. *Masic, A.; Bertinetti, L.; Schuetz, R.; Chang, S.-W.; Metzger, T. H.; Buehler, M. J.; Fratzl, P.: 'Osmotic pressure induced tensile forces in tendon collagen', Nature communications, 6, 5942, 2015.*
18. *Sasaki, N.; Odajima, S.: 'Elongation mechanism of collagen fibrils and force-strain relations of tendon at each level of structural hierarchy', Journal of biomechanics, 29, 1131-1136, 1996.*
19. *Damink, L. O.; Dijkstra, P. J.; Van Luyn, M.; Van Wachem, P.; Nieuwenhuis, P.; Feijen, J.: 'Glutaraldehyde as a crosslinking agent for collagen-based biomaterials', Journal of materials science: materials in medicine, 6, 460-472, 1995.*
20. *Prabakar, S.; Whitby, C. P.; Henning, A. M.; Holmes, G.: 'The Effect of Cloisite (R) Na plus Nanoclay Filler on the Morphology and Mechanical Properties of Loose Leather', Journal of the American Leather Chemists Association, 111, 178-184, 2016.*
21. *Drljaca, A.; Anderson, J.; Spiccia, L.; Turney, T.: 'Intercalation of montmorillonite with individual chromium (III) hydrolytic oligomers', Inorganic Chemistry, 31, 4894-4897, 1992.*
22. *Abollino, O.; Aceto, M.; Malandrino, M.; Sarzanini, C.; Mentasti, E.: 'Adsorption of heavy metals on Na-montmorillonite. Effect of pH and organic substances', Water research, 37, 1619-1627, 2003.*
23. *Bertinetti, L.; Masic, A.; Schuetz, R.; Barbetta, A.; Seidt, B.; Wagermaier, W.; Fratzl, P.: 'Osmotically driven tensile stress in collagen-based mineralized tissues', Journal of the mechanical behavior of biomedical materials, 52, 14-21, 2015.*
24. *Fein, M.; Filachione, E.; Naghski, J.; Harris Jr, E.: 'Tanning with glutaraldehyde III. Combination tannages with chrome', The Journal of the American Leather Chemists Association, 58, 202-221, 1963.*
25. *Liu, Y.; Ma, L.; Gao, C.: 'Facile fabrication of the glutaraldehyde cross-linked collagen/chitosan porous scaffold for skin tissue engineering', Materials science and engineering: c, 32, 2361-2366, 2012.*
26. *Madhan, B.; Muralidharan, C.; Jayakumar, R.: 'Study on the stabilisation of collagen with vegetable tannins in the presence of acrylic polymer', Biomaterials, 23, 2841-2847, 2002.*
27. *Holmgren, S. K.; Bretscher, L. E.; Taylor, K. M.; Raines, R. T.: 'A hyperstable collagen mimic', Chemistry & Biology, 6, 63-70, 1999.*